# Ultrathin polymer membranes with patterned, micrometric pores for organs-on-chips

| | |
|---|---|
| Journal: | *ACS Applied Materials & Interfaces* |
| Manuscript ID | am-2016-05754z |
| Manuscript Type: | Article |
| Date Submitted by the Author: | 13-May-2016 |
| Complete List of Authors: | Pensabene, Virginia; Vanderbilt University, Biomedical Engineering; University of Leeds, School of Electronic and Electrical Engineering<br>Costa, Lino; University of Tennessee Space Institute, Center for Laser Applications<br>Terekhov, Alexander; University of Tennessee Space Institute, Center for Laser Applications<br>Gnecco, Juan; Vanderbilt University Medical Center, Department of Cellular and Molecular Pathology<br>Wikswo, John; Vanderbilt University, Vanderbilt Institute for Integrative Biosystems Research and Education; Vanderbilt University, Department of Physics and Astronomy; Vanderbilt University, Department of Molecular Physiology and Biophysics<br>Hofmeister, William; University of Tennessee Space Institute, Materials Science and Engineering |
| | |

# Ultrathin polymer membranes with patterned, micrometric pores for organs-on-chips

*Virginia Pensabene*[1], Lino Costa[2], Alexander Terekhov[2], Juan S. Gnecco[3], John Wikswo[1,4,5,6]*

*William Hofmeister[2,4]*

[1] Department of Biomedical Engineering; Vanderbilt University, Nashville, TN 37235 USA

[2]Center for Laser Applications, University of Tennessee Space Institute, Tullahoma, TN 37388 USA

[3]Department of Cellular and Molecular Pathology, Vanderbilt University, Nashville, TN 37235 USA

[4]Vanderbilt Institute for Integrative Biosystems Research and Education; Vanderbilt University, Nashville, TN 37235 USA

[5]Department of Physics and Astronomy; Vanderbilt University, Nashville, TN 37235 USA

[6]Department of Molecular Physiology and Biophysics; Vanderbilt University, Nashville, TN 37235 USA

KEYWORDS. Semipermeable ultrathin polymer membranes, microporous ultrathin polymer films, spin coating, microneedles, femtosecond laser machining, polymer replication.

**ABSTRACT**

The *basal lamina* or basement membrane (BM) is a key physiological system that participates in physicochemical signaling between tissue types. Its formation and function are essential in tissue maintenance, growth, angiogenesis, disease progression, and immunology. *In*

*vitro* models of the BM, *e.g.,* Boyden and transwell chambers, are common in cell biology and lab-on-a-chip devices where cells require apical and basolateral polarization. Extravasation, intravasation, membrane transport of chemokines, cytokines, chemotaxis of cells, and other key functions are routinely studied in these models. The goal of the present study was to integrate a semipermeable ultrathin polymer membrane with precisely positioned pores of 2 μm diameter in a microfluidic device with apical and basolateral chambers. We selected poly (L-lactic acid) (PLLA), a transparent biocompatible polymer, to prepare the semipermeable ultrathin membranes. The pores were generated by pattern transfer using a three-step method coupling femtosecond laser machining, polymer replication, and spin coating. Each step of the fabrication process was characterized by scanning electron microscopy to investigate reliability of the process and fidelity of pattern transfer.

In order to evaluate the compatibility of the fabrication method with organs-on-a-chip technology, porous PLLA membranes were embedded in polydimethylsiloxane (PDMS) microfluidic devices and used to grow human umbilical vein endothelial cells (HUVECS) on top of the membrane with perfusion through the basolateral chamber. Viability of cells, optical transparency of membranes and strong adhesion of PLLA to PDMS were observed, thus confirming the suitability of the prepared membranes for use in organs-on-a-chip devices.

## INTRODUCTION

*In vitro* models are an essential part of cell biology. Transwells have been widely adopted for polarized cell and migration assays since Boyden's initial chemotaxis experiment.[1] The promise of organs-on-a-chip technology is essentially to create a more robust model of the complex electrophysicochemical systems that control cell function and fate.[2,3] In static transwells as well as complex microfluidic organ models, a key element is the basil lamina or basement

membrane (BM).[4] This membrane supports diverse epithelial cell types and participates in signaling and transport for the system.[5] In contrast to the static transwell and Boyden chamber devices, microfluidic barrier devices offer the possibility of using physiologically realistic flow of cell culture media so that the resulting shear stresses polarize the endothelial cells on the vascular side of the BM, as might be found in organ-on-chip models of the blood-brain barrier.[6,7] Critical properties of a semipermeable membrane in a microfluidic device include controlled porosity, high species flux, mechanical strength, surface biocompatibility, and optical transparency. Polycarbonate and polyester membranes are the main materials for transwell cell culture and diffusion experiments. These membranes are far thicker than the BM and the transparency is not optimal in bright field light, confounding observation by differential interference contrast. Ultrathin polymer films (nanofilms) are promising candidates for the membrane model system. They are closer in thickness to native BM, are optically transparent and compatible with cell culture.

Nanofilms with thicknesses ranging from tens to hundreds of nanometers belong to an interesting class of polymeric nanomaterials having lateral-dimension-to-thickness ratios that are greater than $10^6$, and unique thickness-dependent interfacial and mechanical properties. In particular, previous studies have revealed that such films can have non-covalent high adhesiveness to surfaces, tunable flexibility and molecular permeability,[8] defined structural color,[9] and mechanical strength,[10] and possibly conductive[11] and magnetic properties.[12] These characteristics make such films a promising solution for multiple applications in the biomedical field. As an example, thanks to their quasi-two-dimensional nature, such nanofilms resemble the *lamina basalis* of the extracellular matrix in human tissues, the ideal structure to direct the cellular organization and function thereby enabling organ regeneration and function.

Nanofilm fabrication techniques are diverse, and include layer-by-layer,[13] Langmuir–Blodgett methods[14] and others. The simplest route to fabricate freestanding and easy-to-handle nanofilms is spin coating from a liquid polymer-solvent solution.[15] In previous works, full characterization of plain nanofilm structures was performed. The adhesion and proliferation of different cell types on poly (lactic acid) (PLLA) nanofilms[16] and polyelectrolytic films[17] was confirmed. We now report on the fabrication and characterization of ultrathin semipermeable PLLA membranes for organs-on-a-chip applications. Herein "semipermeable membranes" refer to membranes with ordered pores of a specific size, distribution and shape that are precisely patterned to allow passage of chemical species and cells of a specific size range, while blocking migration of other cells. The semipermeable membranes function as support for growth of cell layers and as separation between distinct microfluidic chambers.

Existing examples of organs-on-a-chip have used perforated polydimethylsiloxane (PDMS) membranes,[18,19] polycarbonate[7,20] or photoresist membranes.[21,22,23] While the PDMS membranes have the advantages of optical transparency, tunable elastic modulus and can be easily integrated in a monolithic PDMS device, it is still difficult to reduce the thickness of the membrane below 5 μm. Submicron membrane thickness is essential for physical contact and paracrine communication between cells growing on both sides.

The engineered semipermeable ultrathin polymer membranes are an advancement over current solutions. Numerous approaches have been used to fabricate organic semipermeable membranes,[24] such as polymer synthesis[25] and ion track etching of polymers.[26] However, most of these methods have drawbacks, mainly related to random arrangement of pores with a wide size distribution or nanometric/sub-micrometric pore size. Other methods use e-beam lithography and by focused ion beam milling for direct micro- and nanofabrication of the pores on an otherwise

unpatterned polymer sheet.[27,28] These approaches have the advantage of control on the design and arrangement of the pores,[29] but they also present drawbacks, such the length of time and hence cost required for serial, pore-by-pore fabrication of each membrane. Moreover, while direct etching of any polymeric film should be theoretically possible for example by tuning current and voltage of an ion or electron beam, [29] it is practically impossible to drill holes with micrometric diameter through a ~100 nm thin film. The Gaussian distribution of the ion beam and the control of current and milling depth are not sufficient to avoid local polymer melting. Debris from the milling process limits the depth to 10x the diameter of the hole. Furthermore, direct milling of the film would implicate local changes in the film mechanical and structural characteristics and thus increase the risk of breakage and tears in the polymer film.

Alternatively, ultrathin polymer membranes containing precisely patterned micrometric pores can be formed by spin coating assisted deposition of a polymer-solvent solution atop a sacrificial array of spatially ordered polyvinyl-alcohol (PVA) nanoneedles, followed by removal of the sacrificial PVA nanoneedle array. The PVA nanoneedles are formed by PVA replication of an array of surface nanometric pores formed on a fused silica wafer using femtosecond laser machining. The details and suitability of this novel approach are outlined herein for PLLA membranes.

## MATERIALS AND METHODS

### Fabrication of fused silica molds

As a first step towards creating the PVA needle array, a 10 mm × 10 mm regular array of 201×201 pores was patterned on the surface of a 500 µm thick UV grade fused silica wafer (Mark Optics, Inc.) using the single-pulse femtosecond laser machining technique first described

by White, et al.[30] In their 2008 paper, White and co-workers demonstrated that high numerical aperture single-pulse femtosecond laser machining can create uniquely-shaped pores at the surface of fused silica, exhibiting high aspect ratios, with depths that exceed 10 μm and diameters below 200 nm. In the present work, femtosecond laser machining was carried out using the system described by Rajput.[31] A dry microscope objective, namely a Nikon CF Plan Achromat 79173, was used to focus the femtosecond laser beam on the surface of the fused silica wafer. Energy per pulse of 3.2 μJ was used to open each pore. The laser-patterned wafer was soaked first in a 5 M KOH solution at 80°C for 2 hours, and then in de-ionized water also at 80°C for another 2 hours, in order to remove any machining debris. The washed wafer was dried under a stream of nitrogen, and used to prepare PLLA membranes for characterization purposes.

A second fused silica mold, designed to prepare PLLA membranes for use in organs-on-a-chip trials was femtosecond laser machined in a similar way. This mold was patterned with a 16 row x 100 column rectangular array of surface pores. The distance between rows was 400 μm, while the distance between columns was 100 μm, thereby creating pores whose arrangement matched channels in the microfluidic device.

**Preparation of PVA nanoneedle arrays**

Once the femtosecond laser patterned fused silica mold was fabricated, the freestanding polymer nanoneedle arrays were produced using the novel solution-casting mold-replication method recently reported by Rajput and co-workers.[31,32] In the present work, arrays of freestanding polyvinyl alcohol (PVA) nanoneedles (or PVA replicas) were prepared using the water/alcohol-based PVA mold release agent Partall® Film #10 (Rexco). In particular, each fused silica mold containing an array of surface pores was coated with a thin layer of Partall® Film #10 using a foam paintbrush. The layer was exposed to a flow of nitrogen and allowed to

dry (Fig.1a). The resulting ~25 µm thick PVA film with nanoneedles was peeled-off the fused silica mold and mounted on a 22×22 $mm^2$ glass or polyvinyl chloride (PVC) coverslip using double-sided adhesive tape (Fig. 1b).

**Preparation of PLLA membranes**

Spin-coating-assisted deposition of PLLA on the PVA replicas was performed using the same processing parameter values used to prepare plain ~100 nm thin PLLA films reported in previous work[33]. A 10 mg/mL solution of PLLA in dichloromethane (molecular weight 100 kDa; Polysciences, Inc.) was applied to the PVA nanoneedle array and spun at 3000 rpm for 30 s inside a Class 100 clean room (Fig. 1c). The resulting PLLA films were allowed to dry for 1 minute at 80°C and stored in polystyrene Petri dishes.

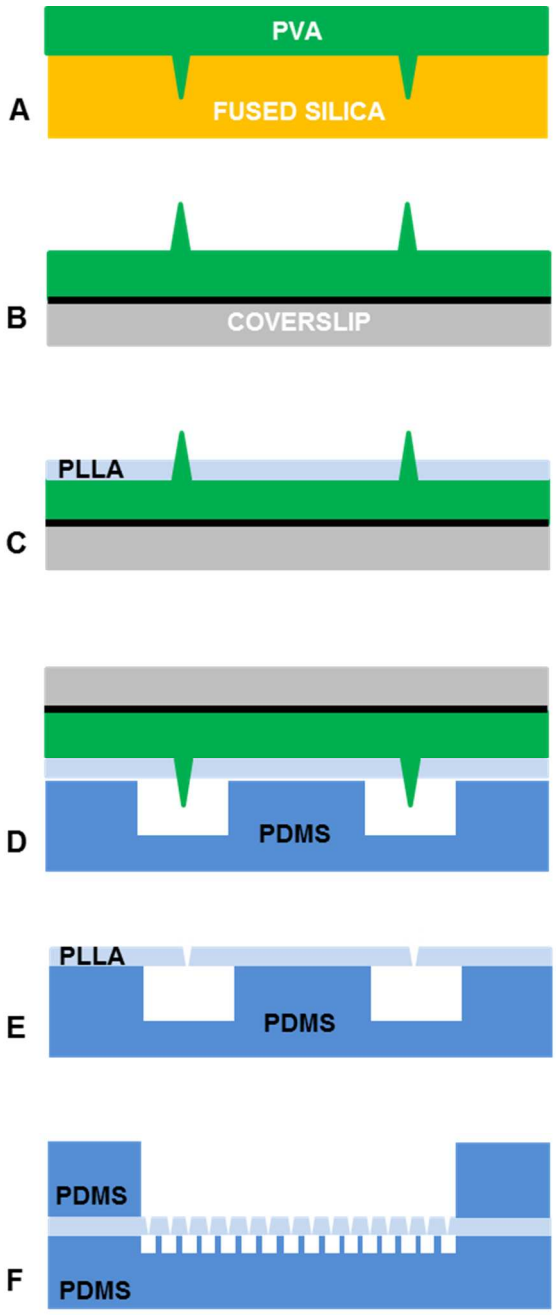


**Fig. 1**- Process for fabrication of a semipermeable ultrathin PLLA membrane. a) PVA microneedle array is created by casting the PVA solution on a fused-silica mold and by allowing the PVA to dry. b) PVA replica is lift-off bonded to coverslip using adhesive tape (black solid line). c) PVA replica is spin coated with PLLA. d) PLLA film is placed in contact and aligned to the PDMS microfluidic layer. e) PLLA film is adherent on the

PDMS layer. f) The final assembled device presents the PLLA barrier between two microfluidic chambers.

**Assembly of microfluidic devices**

A simple two-compartment device was assembled to test the semipermeable PLLA membranes in an organs-on-a-chip assembly. The device consists of two microfabricated layers in polydimethylsiloxane (PDMS, Sylgard® 184 silicone elastomer kit from Dow Corning, MI, USA), produced by SU8 softlithography[34]. Briefly, the bottom layer consists of 16 parallel channels (200 μm width, 100 mm height, 10 mm length, and separated by a 200 μm space), obtained by casting and curing liquid PDMS (10:1) on SU8-2100 mold (from Microchem, MA, USA) fabricated in a Class 100 clean room. The upper chamber was prepared by punching a thick 3 mm layer of PDMS with a sterile disposable 6 mm diameter punch. Ports to access the microfluidic channels were opened by punching 1.59 mm (1/16 inch) diameter holes.

In order to bond a PLLA membrane between the two PDMS layers, the channeled PDMS layer was gently pressed against the PLLA layer formed atop a PVA replica (Fig. 1d). These two pieces were then immersed in de-ionized water for 6 to 12 hours to allow water to gradually dissolve and remove the sacrificial PVA template, leaving behind a semipermeable ultrathin PLLA membrane with precisely patterned micrometer scale pores (Fig. 1e). The resulting PLLA membrane remained adherent to the channeled PDMS layer. The upper PDMS layer chamber and the PLLA membrane were then oxygen-plasma treated (600 mTorr, 100 W, for 45 sec) and finally bonded together (Fig. 1f). Oxygen-plasma treatment renders the exposed surfaces hydrophilic. Once bonded the devices were immediately filled with deionized sterile water and stored at 4°C until used.

**Cell culture, staining and assays**

Human umbilical vein endothelial cells (HUVECS)[35] were isolated from umbilical cord obtained from a de-identified placenta collected from patients who underwent elective cesarean sections between 37 and 39 weeks of gestation. All procedures related to the consent and collection of tissues were approved by the Vanderbilt University Institutional Review Board. Cells were cultured in EBM-2 media supplemented with 10% of fetal bovine serum (Lonza, USA) and with 1% antibiotics/antimycotics. Purity of the isolation was validated by morphological and immunofluorescent staining for CD31 (DAKO, USA) before loading in the devices. Cells were maintained at 37°C in a saturated humidity atmosphere containing 95% air / 5% $CO_2$, and they were sub-cultured before reaching 70% confluence (approximately every 2 days).

After tripsinization and centrifugation, cells were suspended in full medium (2000 cells/μL) and 50 μL were injected in the device. Medium was refreshed in the device every 2 days. Cell growth on the PLLA nanofilm was monitored for 7 days as proof of principle.

Vitality was investigated after 7 days in culture by using NucBlue® Live ReadyProbes® Reagent and NucGreen® Dead 488 ReadyProbes® Reagent (Molecular Probes, R37605 and R37109). 20 μL of staining solutions were added directly to cells in full media and incubated for 20 minutes. NucBlue® Live Cell Stain emits at 460 nm when bound to DNA while NucGreen® Dead 488 reagent is a membrane-impermeable stain DNA of dead cells (excitation/emission at 504/523 nm). Cellular cytoskeleton was visualized by F-actin staining using ActinGreen™ 488 ReadyProbes® Reagent from Molecular Probes. Cells were prepared for staining by 4% paraformaldehyde fixation.

Cells were finally observed with an inverted fluorescent microscope (EVOS, FL Cell Imaging System) and with Image J software (Rasband, W.S., ImageJ, U. S. National Institutes of Health, Bethesda, Maryland, USA).

**Loading of microfluidic devices**

The devices were sterilized by UV irradiation for 30 minutes prior to loading with cell medium and cells. Mimicking the seeding protocol used for cell culture in traditional transwell inserts, the water was replaced with EBM-2 cell-culture media supplemented with 10% of fetal bovine serum (Lonza, USA), first loading the lower microfluidic channels and then the upper chamber. The nanofilm was not coated with any adhesive protein other than that in the media. The wet device was then enclosed in a Petri dish and equilibrated at 37°C for 12 hours inside the incubator.

## RESULTS

**SEM characterization of fused silica molds and PVA replicas**

The surfaces of both the femtosecond laser patterned fused silica mold and the corresponding PVA replica were imaged using a JEOL 6320 field emission scanning electron microscope (SEM). Both samples were sputter-coated with a few nanometers of platinum for successful imaging. An image of a single-pulse femtosecond laser machined pore is shown in Figure 2a. Images of the PVA replica, at various magnifications, are shown in Figures 2b-d.

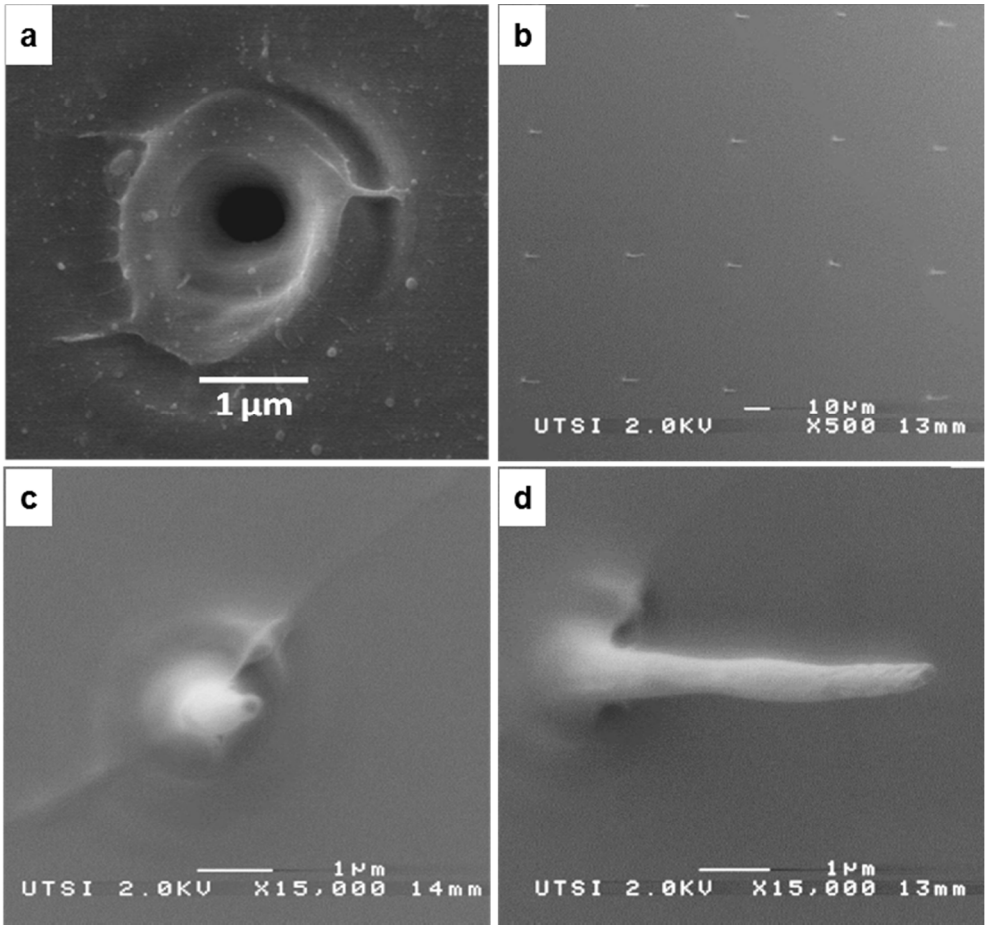


**Figure 2 – Process characterization**. a) SEM image of a femtosecond laser machined pore on the surface of a fused silica wafer. The pore was opened using a single 3.2 µJ, 790 ηm, 160 femtosecond laser pulse; b) SEM image of a PVA replica (Pt coated, 45° stage tilt). c) A single PVA nanoneedle with a final length of 10 µm. d) same PVA nanoneedle at 30° stage tilt.

**SEM characterization of PLLA membrane**

The effectiveness of the spin coating of PLLA on the PVA microneedle array is apparent in Fig. 3d: the PLLA solution spread and coated the full surface of the replica. Due to the high

aspect ratio of the PVA needles and lack of wettability, the tips of the needles were not completely covered during the spin coating (Supporting information, Fig. S1).

The sacrificial layer PVA was dissolved by immersion in de-ionized water, and once removed, the PVA needle sites become open pores in the PLLA nanofilm membrane. While in this report, the PLLA film was transfer bonded to the PDMS, the hydrophobic PLLA film can be floated freestanding on the water surface for visualization (Fig. 3a). The patterned pores can be visualized in bright field once the film is collected and dried on a flat surface, such as a silicon wafer or a glass coverslip (Fig. 3b-c). The PLLA nanofilm replicates perfectly the surface morphology and any irregularity of the PVA replica, including the features imposed by the laser in the original silica mold (Fig. 3d).

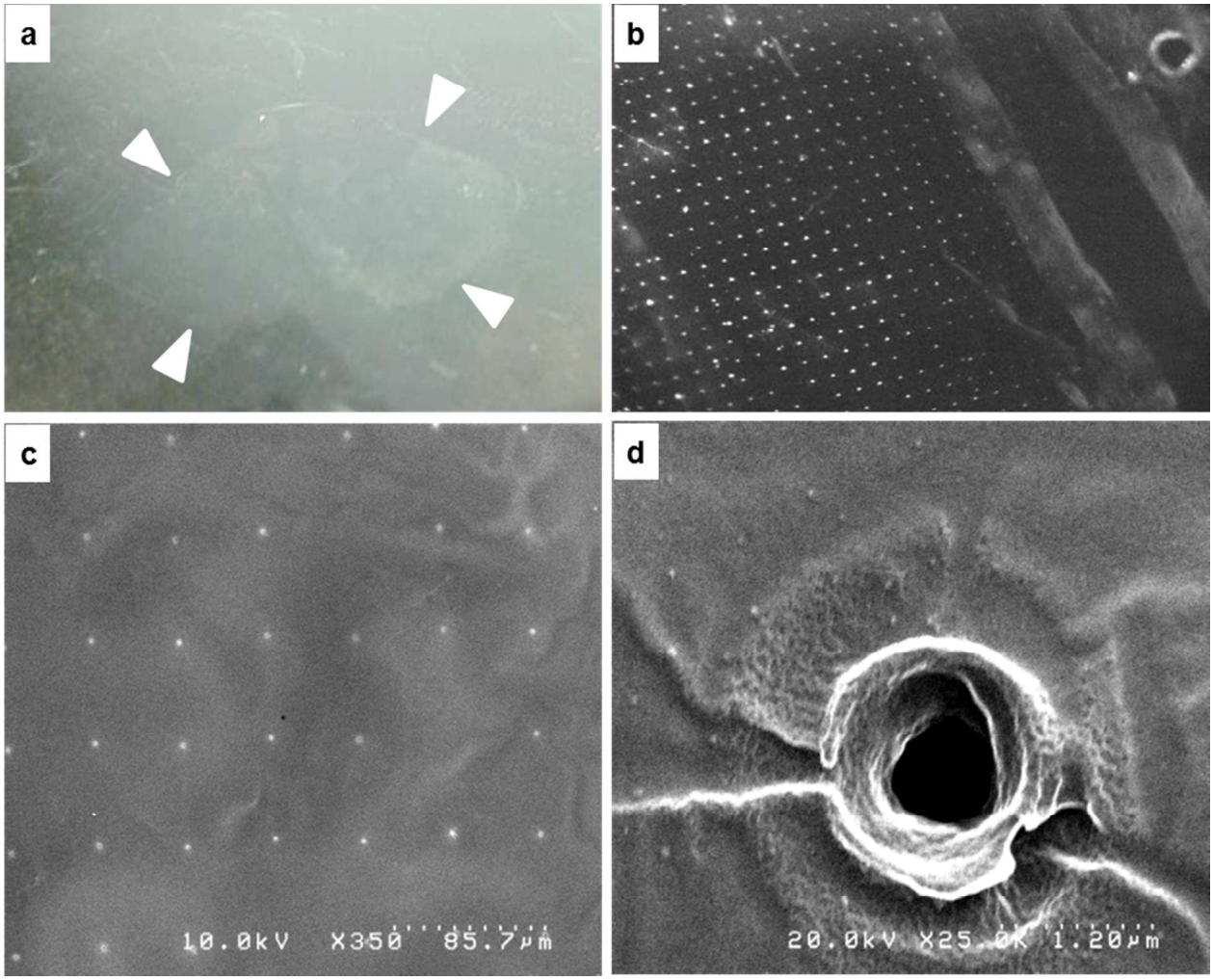


**Fig. 3 – Characterization of PLLA film.** a) film floating on water surface after the PVA template dissolved (film edges highlighted with white arrows); b) optical microscope image of the film (holes appear as white dots); c) the array of holes in the film are visualized with the SEM (2 nm gold coating); d) A detail of a single hole in the PLLA film.

Different views of a PLLA semipermeable membrane bonded to the channeled, bottom PDMS layer are shown in Fig. 4.

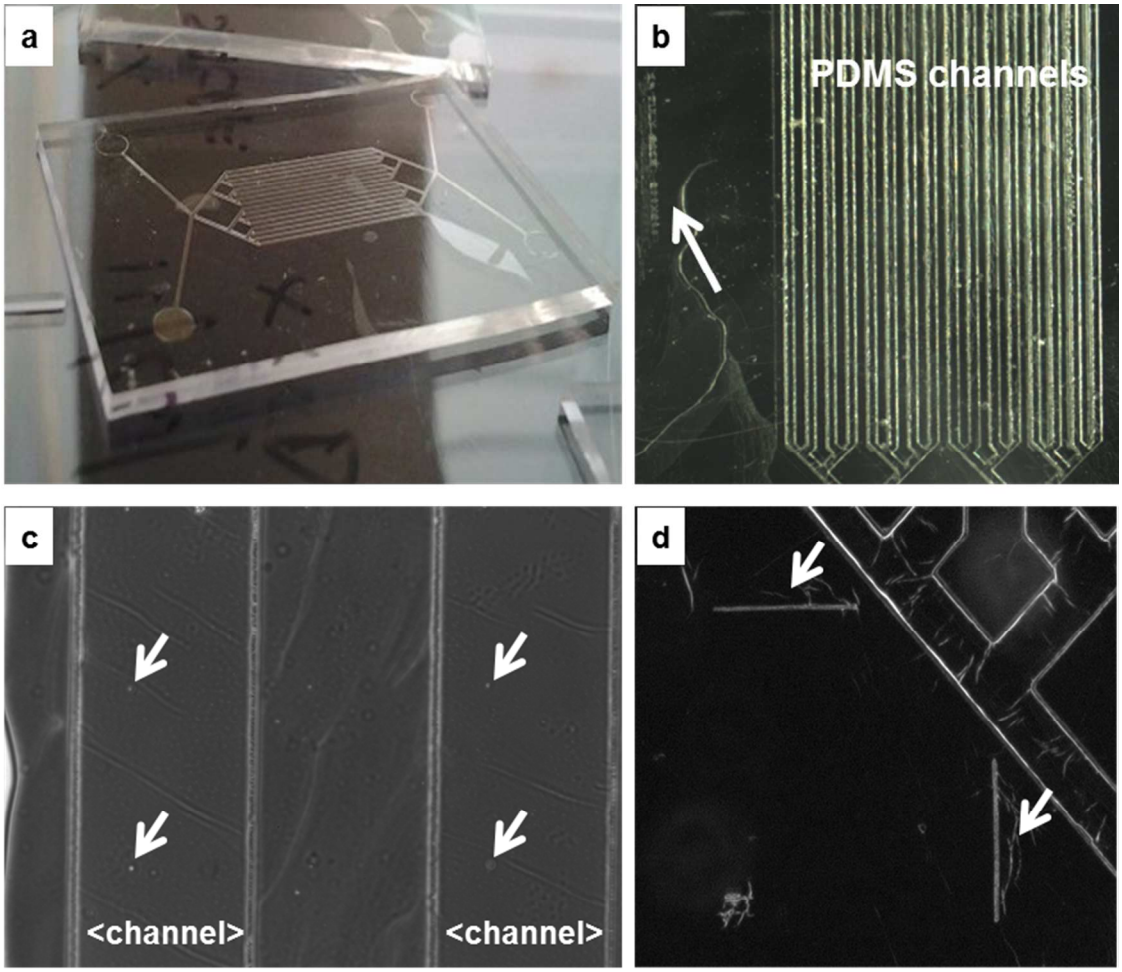


**Fig. 4 - Device assembly.** a) PLLA film adherent to channeled, bottom PDMS layer; b) PLLA film on a channeled PDMS bottom layer with arrow pointing to the lateral identification label; c) magnified view of Figure 4b showing a group of four micrometric pores in the PLLA membrane laying above the 200 μm-wide microfluidic channels in the PDMS layer; d) alignment features.

**Device Assembly**

The PLLA membrane bonded wrinkle-free to the channeled PDMS layer (Fig. 4a). The sixteen rows of micrometric pores of the PLLA membrane aligned precisely above the sixteen-microfluidic channels. The sacrificial PVA layer provides a means of handling the nanofilm and

mounting the film on the channeled PDMS layer preventing damage to the film; a key concern in manipulation of the ultrathin membrane.

Since both PDMS and PLLA are optically transparent, alignment of various components was done under a stereomicroscope. Together with the pattern of surface pores, the original silica mold has femtosecond laser machined surface alignment marks and a lateral identification label (Fig. 4.b-d); these microscopic features transfer to the PVA and PLLA films and serve as alignment guides during device assembly.

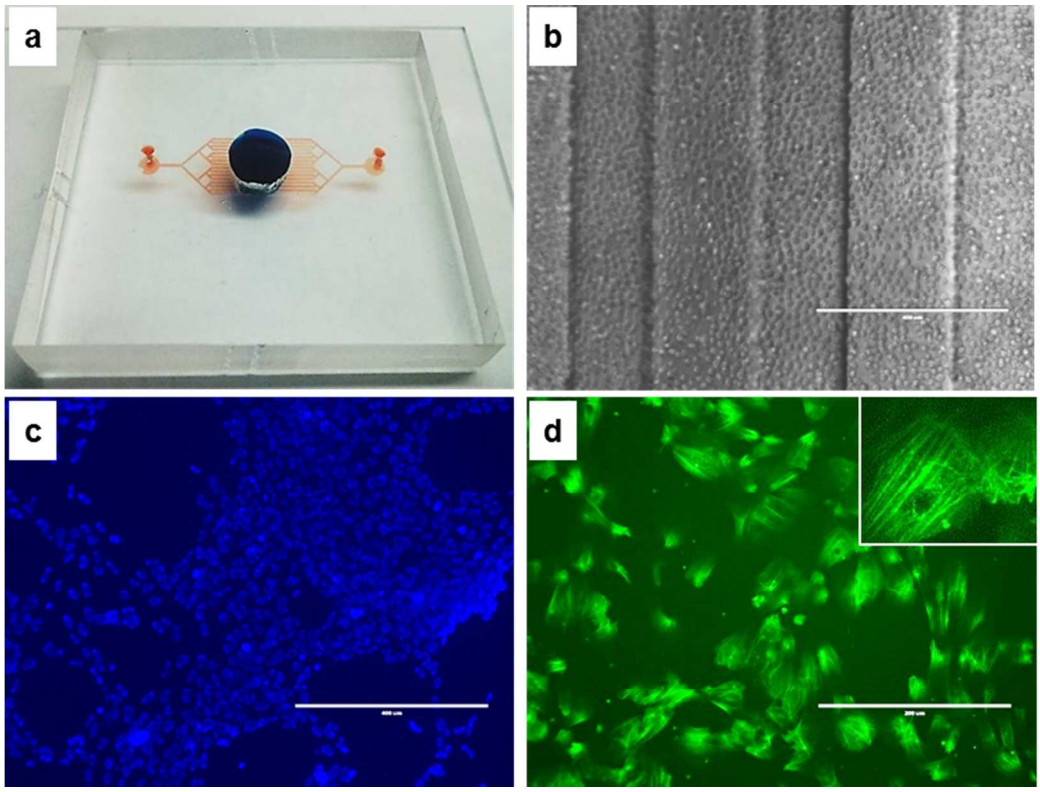


**Fig. 5 - Cells adhesion in the device.** a) Full device (blue dye for upper chamber volume, red dye for the lower, channeled chamber volume); b) HUVECs at the time of loading (D0, 4x, ph); c) LIVE/DEAD staining of the cells (green for dead cells, blue for live cells, scale bar 400 μm); d) actin staining of HUVECs inside the device (green for actin, scale bar 400 μm; inset at 40x).

We observed that the PLLA membrane adhered tightly to the channeled PDMS layer and did not collapse inside the channels (Fig. 5a). Cells were then seeded directly on the PLLA membrane in the upper chamber without prior coating of the surface. Approximately 100,000 cells were seeded at Day 0 in the device, filling the upper chamber without leakage between the layers. It was possible to observe the cell behavior and monitor growth by optical microscopy due to the transparency of the PLLA membrane in bright field.

Oxygen plasma treatment did not adversely affect the biological properties of the PLLA film surfaces; the grow rate and cell morphology of the cells on PLLA inside the device were comparable to the control flask. As shown in Fig. 5c-d, cells proliferate rapidly in the device and with very low mortality (below 1%). The media of the two chambers was replaced every 48 hours and after 7 days the adhesion of the cells on the semipermeable PLLA membrane was confirmed by F-actin staining (Fig. 5.d). Cells were trypsinazed and the suspensions from the two chambers were collected to measure the amount of cells by using a cell counter. Cells were found only in medium from the upper chamber, thus proving that the size of the pores did not exceed the nominal value of 1 μm in diameter (data not shown). At the same time, the permeability of the membrane was confirmed by 150 kDa FITC-dextran diffusion measurements (as reported in Supporting information, Figure S2).

## DISCUSSION AND CONCLUSIONS

Fabrication of biocompatible, transparent, semipermeable ultrathin polymer membranes with precisely patterned micropores is difficult by perforation using e-beam lithography, focused ion beam milling, or laser micromachining. Additionally, such processes lack production scalability. Forming membranes using a molding approach is also difficult to implement. First of

all, the polymer melt, polymer precursor, or the polymer-solvent solution being used must have sufficiently low viscosity to spread and fill the surface of the mold completely and homogeneously, without leaving a residual layer on top of the mold micropillars. Mechanical peeling of the membrane is problematic due to the thickness of the membrane. Once released from the mold, the membrane must be transferred and precisely attached to the microfluidic device and without any wrinkles and folds.

The method reported in this paper provides a quick, repeatable and convenient route to prepare multiple copies of the desired membranes. First, the direct one-step femtosecond laser machining of the fused silica molds can be carried out at kilohertz rates. With the current system, this translates to patterning a regular array of four million surface pores inside a one square centimeter area in less than one hour. Molds can be prepared with a distance between pores as small as 2 μm. The construction of the silica mold with alignment marks allows the user to control the size and location of each pore, and more importantly, the density of pores. While in this demonstration, each microfluidic channel had a single line of 100 pores each separated by 100 μm, the ability to separate pores by as little as 2 μm would allow us to have tens of thousands of pores in each channel. The ability to control the location of pores means that the femtosecond laser drilling need not be wasted on regions of membrane sandwiched between solid PDMS, and the presence of pores and any associated surface irregularities is avoided in such regions where PDMS bonding is critical to avoids leaks and channel cross-talk.

Chemically inert and mechanically hard, the fused silica mold can be used to prepare thousands of PVA replicas. The PVA formulation used does not stick to fused silica. Each PVA replica precisely and repeatedly duplicates all the features of the mold, yielding straight, standing, and aligned high aspect-ratio nanoneedles. PVA replicas can be produced relatively

quickly (15-30 minutes) and the mold can be easily cleaned from residual traces of PVA by hot water. The water-solubility and organic solvent-resistance of PVA makes it a suitable sacrificial material to use as template in preparing semipermeable membranes for many organic solvent-soluble polymers of interest. Finally, the PVA template provides a convenient vehicle to transfer, align and attach the ultrathin membrane to the microfluidic device without introducing undesirable wrinkles or folds in the final assembly.

While the selection of biocompatible polymers is wide and the fabrication of films with micron thicknesses can be achieved with several methods, handling of a perforated thin membrane represents a technological challenge. In this work we selected PLLA since its biocompatibility is well demonstrated. Furthermore, the PVA sacrificial layer is fundamental for handling and positioning of the ultrathin membrane PLLA: while an unpatterned sacrificial layer is traditionally used to release positioning polymeric films from their support, for example in stretchable and epidermal electronics[33,34], in this case the dissolvable PVA includes not only the needles but also temporary labels and frames to align the pattern of needles with the microfabricated channels in the PDMS.

The semipermeable property of these PLLA membrane guarantees the possibility to separate two fluidic compartments and to select the size of particulates (*i.e.,* cells versus macromolecules) able to pass through the pores. This is a key characteristic in lab-on-a-chip technology, where cellular extravasation and passage of chemical species between communicating compartments need to be controlled. Organs-on-a-chip seeks to understand complex processes; *e.g.,* organ development, embryogenesis, tumor metastasis, and leukocyte infiltration that are regulated by cellular responses to multiple (competing) chemokines as well as autocrine feedback loops, cell-cell interactions, and mechanical stress. The result outlined

herein of a scalable, tunable semipermeable nanofilm membrane will contribute to the success of organs-on-a-chip models and enable more faithful recapitulation of *in vivo* conditions.

## ASSOCIATED CONTENT

**Supporting Information**. This section provides additional images of PVA replicas coated with PLLA and closer view of the PVA needles after coating. Additionally, the results of the permeability measurements are summarized. This material is available free of charge via the Internet at http://pubs.acs.org.

## AUTHOR INFORMATION

**Corresponding Author**

*Virginia Pensabene, virginia.pensabene@vanderbilt.edu, Vanderbilt University

C1136 Medical Center North, Nashville, TN 37235, (615)-343-8978.

### Author Contributions

The manuscript was written through contributions of all authors. All authors have given approval to the final version of the manuscript.

### Funding Sources

This work was supported by the Tennessee Higher Education Commission through a grant to the Center for Laser Applications, University of Tennessee Space Institute.

Research reported in this publication was supported in part by the National Center for Advancing Translational Sciences of the NIH under Award Nos.UH2TR000491 and UH3TR000491 and the Vanderbilt Institute for Integrative Biosystems Research and Education. The content is solely the

responsibility of the authors and does not necessarily represent the official views of the funding agencies and organizations.

## ACKNOWLEDGMENT

The authors thank Dr. Brian Canfield for help in developing the LabView code used to operate the femtosecond laser micromachining facility. Additionally, the authors acknowledge Prof. Anthony Hmelo for the use of the SEM microscope at the Vanderbilt Institute of Nanoscale Science and Engineering.

## ABBREVIATIONS

poly (L-lactic acid) (PLLA)

polyvinyl-alcohol (PVA)

basement membrane (BM)

polydimethylsiloxane (PDMS)

human umbilical vein endothelial cells (HUVECS)

polyvinyl chloride (PVC)

## REFERENCES

1. Boyden, S., The chemotactic effect of mixtures of antibody and antigen on polymorphonuclear leucocytes. *The Journal of Experimental Medicine* **1962,** *115* (3), 453-466.

2. Ingber, D. E., Reverse Engineering Human Pathophysiology with Organs-on-Chips. *Cell* **2016,** *164* (6), 1105-1109.

3. Wikswo, J.P., The relevance and potential roles of microphysiological systems in biology and medicine. *Exp.Biol.Med.* **2014,** 239:1061-1072, 2014.

4. Huh, D., Hamilton, G. A., Ingber, D. E., From 3D cell culture to organs-on-chips. *Trends in Cell Biology* **2011,** *21* (12), 745-754.

5. McCaffrey, L. M., Macara, I. G., Epithelial organization, cell polarity and tumorigenesis. *Trends in Cell Biology* **2011,** *21* (12), 727-735.

6. Griep, L. M., Wolbers, F., de Wagenaar, B., ter Braak, P. M., Weksler, B. B., Romero, I. A. , Couraud, P. O., Vermes, I., van der Meer, A. D. , van den Berg, A., BBB ON CHIP: Microfluidic platform to mechanically and biochemically modulate blood-brain barrier function. *Biomed.Microdevices* **2013,** 15 (1):145-150.

7. Brown, J.A., Pensabene, V., Markov, D.A., Allwardt, V., Neely, M.D., Shi M., Britt, C.M., Hoilett, O.S., Yang, Q., Brewer, B.M., Samson, P.C., McCawley, L.J., Webb, D.J., Li, D., Bowman, A.B., Reiserer, R.S.,Wikswo, J.P., Recreating blood-brain barrier physiology and structure on chip: A novel neurovascular microfluidic bioreactor. *Biomicrofluidics* **2015,** 9:Article 0541248. Okamura, Y., Kabata, K., Kinoshita, M., Saitoh, D., Takeoka, S., Free-Standing Biodegradable Poly(lactic acid) Nanosheet for Sealing Operations in Surgery. *Advanced Materials* **2009,** *21* (43), 4388-4392.

9. Fujie, T., Okamura, Y., Takeoka, S., Selective surface modification of free-standing polysaccharide nanosheet with micro/nano-particles identified by structural color changes. *Colloids and Surfaces A: Physicochemical and Engineering Aspects* **2009,** *334* (1–3), 28-33.

10. Markutsya, S., Jiang, C. Y., Pikus, Y., Tsukruk, V. V., Freely suspended layer-by-layer nanomembranes: Testing micromechanical properties. *Advanced Functional Materials* **2005,** *15* (5), 771-780.

11. Zucca, A., Yamagishi, K., Fujie, T., Takeoka, S., Mattoli, V., Greco, F., Roll to roll processing of ultraconformable conducting polymer nanosheets. *Journal of Materials Chemistry C* **2015,** *3* (25), 6539-6548.

12. Taccola, S., Desii, A., Pensabene, V., Fujie, T., Saito, A., Takeoka, S., Dario, P., Menciassi, A., Mattoli, V., Free-Standing Poly(L-lactic acid) Nanofilms Loaded with Superparamagnetic Nanoparticles. *Langmuir* **2011,** *27* (9), 5589-5595.

13. Jiang, C. Y.; Tsukruk, V. V., Freestanding nanostructures via layer-by-layer assembly. *Advanced Materials* **2006,** *18* (7), 829-840.

14. Endo, H., Kado, Y., Mitsuishi, M., Miyashita, T., Fabrication of free-standing hybrid nanosheets organized with polymer Langmuir-Blodgett films and gold nanoparticles. *Macromolecules* **2006,** *39* (16), 5559-5563.

15. Cho, J., Char, K., Hong, J. D., Lee, K. B., Fabrication of highly ordered multilayer films using a spin self-assembly method. *Advanced Materials* **2001,** *13* (14), 1076-+.

16. Ricotti, L., Taccola, S., Pensabene, V., Mattoli, V., Fujie, T., Takeoka, S.; Menciassi, A.; Dario, P., Adhesion and proliferation of skeletal muscle cells on single layer poly(lactic acid) ultra-thin films. *Biomedical Microdevices* **2010,** *12* (5), 809-819.

17. Ricotti, L., Taccola, S., Bernardeschi, I., Pensabene, V., Dario, P., Menciassi, A., Quantification of growth and differentiation of C2C12 skeletal muscle cells on PSS-PAH-based polyelectrolyte layer-by-layer nanofilms. *Biomedical Materials* **2011,** *6* (3).

18. Kim, H. J., Ingber, D. E., Gut-on-a-Chip microenvironment induces human intestinal cells to undergo villus differentiation. *Integrative Biology* **2013,** *5* (9), 1130-1140.

19. Kim, H. J., Huh, D., Hamilton, G., Ingber, D. E., Human gut-on-a-chip inhabited by microbial flora that experiences intestinal peristalsis-like motions and flow. *Lab on a Chip* **2012,** *12* (12), 2165-2174.

20. Booth, R., Kim, H., Characterization of a microfluidic *in vitro model* of the blood-brain barrier (mu BBB). *Lab on a Chip* **2012,** *12* (10), 1784-1792.

21. Esch, M. B., Sung, J. H., Yang, J., Yu, C. H., Yu, J. J., March, J. C., Shuler, M. L., On chip porous polymer membranes for integration of gastrointestinal tract epithelium with microfluidic 'body-on-a-chip' devices. *Biomedical Microdevices* **2012,** *14* (5), 895-906.

22. Ornoff, D. M., Wang, Y., Allbritton, N. L., Characterization of freestanding photoresist films for biological and MEMS applications. J.Micromech.Microeng. 23 (2):Article 025009, 2013.

23. Kim, M. Y., Li, D. J., Pham, L. K., Wong, B. G., Hui, E. E., Microfabrication of high-resolution porous membranes for cell culture. *J.Membr.Sci.* **2014,** *452,* 460-469.

24. Ulbricht, M., Advanced functional polymer membranes. *Polymer* **2006,** *47* (7), 2217-2262.

25. Uragami, T., Naito, Y., Sugihara, M., Studies on synthesis and permeability of special polymer membranes .39. permeation characteristics and structure of polymer blend membranes from poly(vinylidene fluoride) and poly(ethylene glycol). *Polymer Bulletin* **1981,** *4* (10), 617-622.

26. Martin, C. R., Nishizawa, M., Jirage, K., Kang, M., Investigations of the transport properties of gold nanotubule membranes. *Journal of Physical Chemistry B* **2001,** *105* (10), 1925-1934.

27. Kim, M. J., Wanunu, M., Bell, D. C., Meller, A., Rapid fabrication of uniformly sized nanopores and nanopore arrays for parallel DNA analysis. *Advanced Materials* **2006,** *18* (23), 3149-3153.

28. Kuiper, S., van Rijn, C. J. M., Nijdam, W., Elwenspoek, M. C., Development and applications of very high flux microfiltration membranes. *Journal of Membrane Science* **1998,** *150* (1), 1-8.

29. Adiga, S. P., Jin, C. M., Curtiss, L. A., Monteiro-Riviere, N. A., Narayan, R. J., Nanoporous membranes for medical and biological applications. *Wiley Interdisciplinary Reviews-Nanomedicine and Nanobiotechnology* **2009,** *1* (5), 568-581.

30. White, Y. V., Li, X. X., Sikorski, Z., Davis, L. M.; Hofmeister, W., Single-pulse ultrafast-laser machining of high aspect nano-holes at the surface of SiO2. *Optics Express* **2008,** *16* (19), 14411-14420.

31. Rajput, D., Costa, L., Lansford, K., Terekhov, A., Hofmeister, W., Solution-Cast High-Aspect-Ratio Polymer Structures from Direct-Write Templates. *ACS Appl. Mater. Interfaces* **2013,** *5* (1), 1-5.

32. *Optofluidics : fundamentals, devices, and applications*. New York : McGraw-Hill: New York, 2010.

33. Pensabene, V., Patel, P. P., Williams, P., Cooper, T. L., Kirkbride, K. C., Giorgio, T. D., Tulipan, N. B., Repairing Fetal Membranes with a Self-adhesive Ultrathin Polymeric Film: Evaluation in Mid-gestational Rabbit Model. *Annals of Biomedical Engineering* **2015,** *43* (8), 1978-1988.

34. Tang, S.K.Y., Whitesides, G.M., Basic Microfluidic and Soft Lithographic Techniques, in Optofluidics: Fundamentals, Devices, and Applications, Fainman, Y., Psaltis, D.,

Yang, C., Chapter 2, pp.15, 2010 The McGraw-Hill Companies, Inc. ISBN: 9780071601566,

35. Baudin, B., Bruneel, A., Bosselut, N., Vaubourdolle, M., A protocol for isolation and culture of human umbilical vein endothelial cells. *Nature Protocols* **2007,** *2* (3), 481-485.

36. Jeong, J. W., Yeo, W. H., Akhtar, A., Norton, J. J. S., Kwack, Y. J., Li, S., Jung, S. Y., Su, Y. W., Lee, W., Xia, J., Cheng, H. Y., Huang, Y. G., Choi, W. S., Bretl, T., Rogers, J. A., Materials and Optimized Designs for Human-Machine Interfaces Via Epidermal Electronics. *Advanced Materials* **2013,** *25* (47), 6839-6846.

37. Zucca, A., Cipriani, C., Sudha, Tarantino, S., Ricci, D., Mattoli, V., Greco, F., Tattoo Conductive Polymer Nanosheets for Skin-Contact Applications. *Advanced Healthcare Materials* **2015,** *4* (7), 983-990.

## Supporting Information

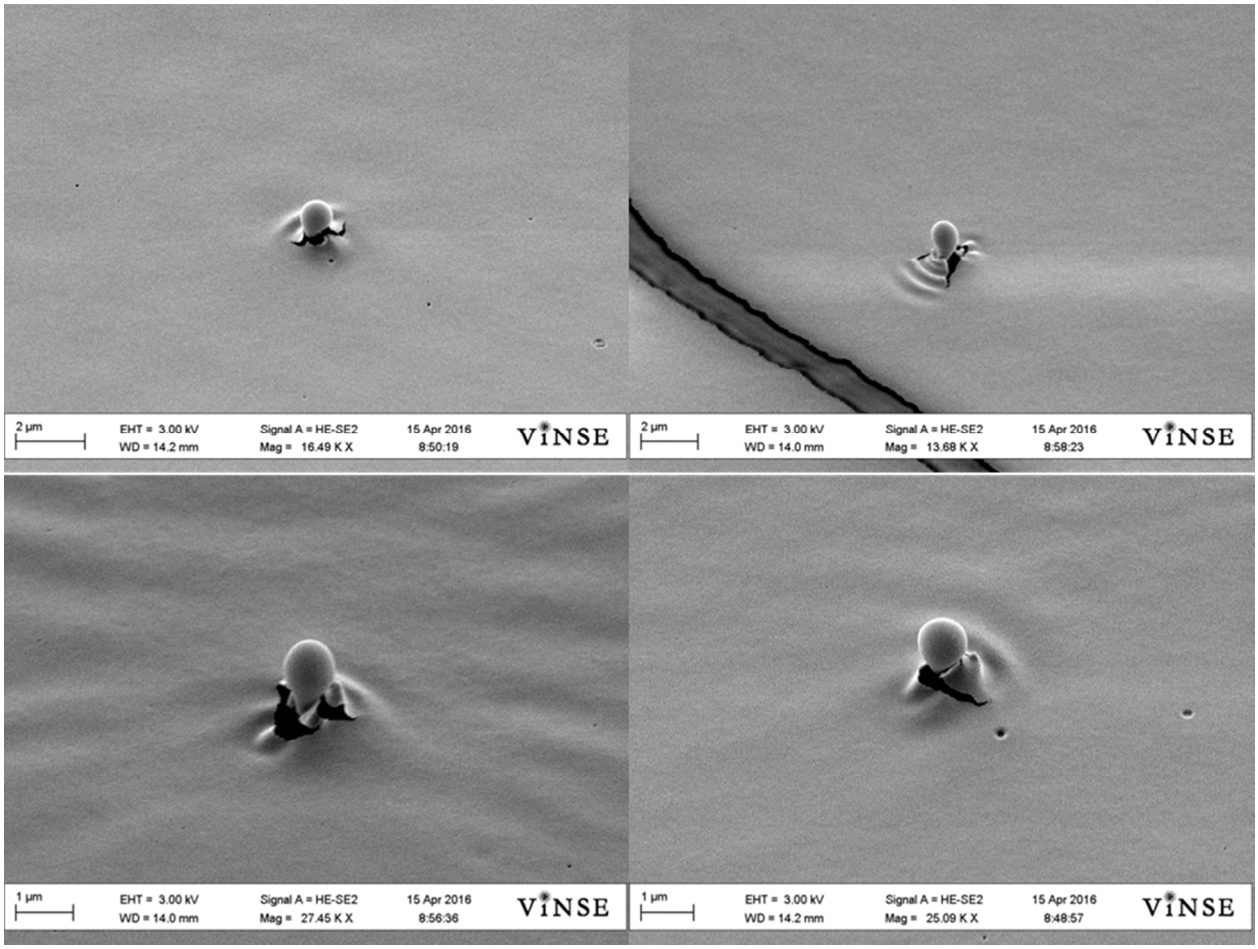


**Figure S1. SEM images of PLLA coated PVA nanowires (Pt coated samples, 30° stage tilt)**

**Permeability of the PLLA nanofilms:**

Diffusion of FITC dextran (70 kDa molecular weight, Sigma Aldrich, USA) through the perforated PLLA membranes was measured by using a UV-Vis Spectrophotometer (Varian Cary 50, Agilent Technologies, Santa Clara, CA).

The experiment was performed in a 96-well plate. Five devices were assembled, following the protocols described in the Materials and Methods section, each one integrating one PLLA perforated membrane. FITC dextran solution (2 mg/mL in MilliQ water) was used to fill

the upper chamber of the device, while the lower channels were filled with MilliQ water. Liquid from the lower channels was collected after 6 hours. One additional device was assembled with a PLLA membrane prepared with the same process parameters on a flat silicon wafer, which thus did not have holes and was not permeable.

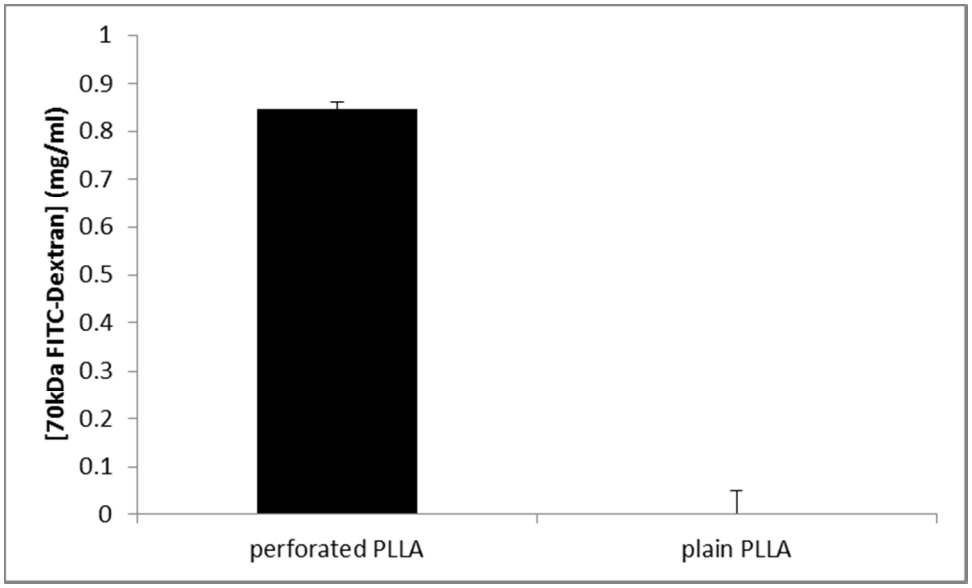


**Figure S2. Permeability of PLLA membranes to FITC-dextran.**